ornl

OAK
RIDGE
NATIONAL
LABORATORY

UNION
CARBIDE

NUREG/CR-3492
Volume 1
ORNL/TM-8921/V1

High-Temperature Gas-Cooled Reactor Safety Studies for the Division of Accident Evaluation Quarterly Progress Report, January 1—March 31, 1983

S. J. Ball
J. C. Cleveland
J. C. Conklin
R. M. Harrington
T. B. Lindemer
I. Siman-Tov

Prepared for the U.S. Nuclear Regulatory Commission
Office of Nuclear Regulatory Research
Under Interagency Agreements DOE 40-551-75 and 40-552-75

OPERATED BY
UNION CARBIDE CORPORATION
FOR THE UNITED STATES
DEPARTMENT OF ENERGY

Printed in the United States of America. Available from
National Technical Information Service
U.S. Department of Commerce
5285 Port Royal Road, Springfield, Virginia 22161

Available from
GPO Sales Program
Division of Technical Information and Document Control
U.S. Nuclear Regulatory Commission
Washington, D.C. 20555

NUREG/CR-3492
Volume 1
ORNL/TM-8921/V1
Dist. Category R8

HIGH-TEMPERATURE GAS-COOLED REACTOR SAFETY STUDIES FOR THE DIVISION OF ACCIDENT EVALUATION QUARTERLY PROGRESS REPORT, JANUARY 1–MARCH 31, 1983

S. J. Ball, Manager
J. C. Cleveland
J. C. Conklin
R. M. Harrington
T. B. Lindemer
I. Siman-Tov

Manuscript Completed — October 19, 1983
Date Published — November 1983

NOTICE This document contains information of a preliminary nature. It is subject to revision or correction and therefore does not represent a final report.

Prepared for the
U.S. Nuclear Regulatory Commission
Office of Nuclear Regulatory Research
Under Interagency Agreement DOE 40-551-75 and 40-552-75

NRC FIN No. B0122

Prepared by the
OAK RIDGE NATIONAL LABORATORY
Oak Ridge, Tennessee 37831
operated by
UNION CARBIDE CORPORATION
for the
DEPARTMENT OF ENERGY
under Contract No. W-7405-eng-26

CONTENTS

PRIOR HTGR SAFETY REPORTS

Quarterly Progress Reports

Ending date	Designation
September 30, 1974	ORNL/TM-4798
December 31, 1974	ORNL/TM-4805, Vol. IV
March 31, 1975	ORNL/TM-4914, Vol. IV
June 30, 1975	ORNL/TM-5021, Vol. IV
September 30, 1975	ORNL/TM-5128
December 31, 1975	ORNL/TM-5255
March 31, 1976	ORNL/NUREG/TM-13
June 30, 1976	ORNL/NUREG/TM-43
September 30, 1976	ORNL/NUREG/TM-66
December 31, 1976	ORNL/NUREG/TM-96
March 31, 1977	ORNL/NUREG/TM-115
June 30, 1977	ORNL/NUREG/TM-138
September 30, 1977	ORNL/NUREG/TM-164
December 31, 1977	ORNL/NUREG/TM-195
March 31, 1978	ORNL/NUREG/TM-221
June 30, 1978	ORNL/NUREG/TM-233
September 30, 1978	ORNL/NUREG/TM-293
December 31, 1978	ORNL/NUREG/TM-314
March 31, 1979	ORNL/NUREG/TM-336
June 30, 1979	ORNL/NUREG/TM-356
September 30, 1979	ORNL/NUREG/TM-366
December 31, 1979	ORNL/NUREG/TM-383
March 31, 1980	ORNL/NUREG/TM-397
June 30, 1980	ORNL/NUREG/TM-415
September 30, 1980	ORNL/NUREG/TM-429
December 31, 1980	ORNL/TM-7809
March 31, 1981	ORNL/TM-7889
June 30, 1981	ORNL/TM-8091
September 30, 1981	ORNL/TM-8128
December 31, 1981	ORNL/TM-8260
March 31, 1982	ORNL/TM-8443/V1
June 30, 1982	ORNL/TM-8443/V2
September 30, 1982	ORNL/TM-8443/V3
December 31, 1982	ORNL/TM-8443/V4

Topical Reports

S. J. Ball, *ORECA-I: A Digital Computer Code for Simulating the Dynamics of HTGR Cores for Emergency Cooling Analyses*, ORNL/TM-5159 (April 1976).

T. W. Kerlin, *HTGR Steam Generator Modeling*, ORNL/NUREG/TM-16 (July 1976).

R. A. Hedrick and J. C. Cleveland, *BLAST: A Digital Computer Program for the Dynamic Simulation of the High Temperature Gas Cooled Reactor Reheater-Steam Generator Module*, ORNL/NUREG/TM-38 (August 1976).

J. C. Cleveland, *CORTAP: A Coupled Neutron Kinetics-Heat Transfer Digital Computer Program for the Dynamic Simulation of the High Temperature Gas Cooled Reactor Core*, ORNL/NUREG/TM-39 (January 1977).

J. C. Cleveland et al., *ORTAP: A Nuclear Steam Supply System Simulation for the Dynamic Analysis of High Temperature Gas Cooled Reactor Transients*, ORNL/NUREG/TM-78 (September 1977).

S. J. Ball et al., *Evaluation of the General Atomic Codes TAP and RECA for HTGR Accident Analyses*, ORNL/NUREG/TM-178 (May 1978).

J. C. Conklin, *ORTURB: A Digital Computer Code to Determine the Dynamic Response of the Fort St. Vrain Reactor Steam Turbines*, ORNL/NUREG/TM-399 (March 1981).

S. J. Ball et al., *Summary of ORNL Work on NRC-Sponsored HTGR Safety Research, July 1974–September 1980*, ORNL/TM-8073 (March 1982).

FOREWORD

High-temperature gas-cooled reactor safety studies at Oak Ridge National Laboratory are sponsored by the Division of Accident Evaluation (formerly the Division of Reactor Safety Research), which is part of the Office of Nuclear Regulatory Research of the Nuclear Regulatory Commission.

This report covers work performed from January 1–March 31, 1983. Previous quarterly reports and topical reports published to date are listed on pages v and vi. Copies of the reports are available from the Technical Information Center, U.S. Department of Energy, Oak Ridge, TN 37831.

HIGH-TEMPERATURE GAS-COOLED REACTOR SAFETY STUDIES FOR THE DIVISION OF ACCIDENT EVALUATION QUARTERLY PROGRESS REPORT, JANUARY 1—MARCH 31, 1983

S. J. Ball, Manager

J. C. Cleveland R. M. Harrington
J. C. Conklin T. B. Lindemer
I. Siman-Tov

ABSTRACT

Work continued on high-temperature gas-cooled reactor safety research directed towards both the Fort St. Vrain and 2240-MW(t) lead plant reactors. Code development and verification activities addressed simulations of unrestricted core heatup accidents, steam generator and turbine-plant perturbations, and fission-product redistribution during severe accidents. Analyses and sensitivity studies of the lead plant thermal response were made for postulated severe accidents, and partial pressures of pertinent reactor materials were calculated for the resulting severe accident environment.

---

1. HTGR SYSTEMS AND SAFETY ANALYSIS

S. J. Ball

Work for the Division of Accident Evaluation (formerly Reactor Safety Research) under the High-Temperature Gas-Cooled Reactor (HTGR) Systems and Safety Analysis Program began in July 1974, and progress is reported quarterly. Work during this quarter included development of the Oak Ridge National Laboratory (ORNL) HTGR Safety Codes, their applications to accident analyses both for the Fort St. Vrain (FSV) and lead plant HTGRs, and studies of fission-product (FP) release and transport during severe accidents.

1.1 Development of the ORECA Code for Simulating FSV Reactor Core Transients

R. M. Harrington

Development continued on the ORECA-FSV code[1] for modeling FSV long-term unrestricted core heatup accident (UCHA) scenarios. The task of installing routines to calculate the temperatures of the prestressed concrete reactor vessel (PCRV) liner, concrete, and liner cooling system (LCS) was initiated. Prior to this point, the ORECA-FSV code used the simplifying assumption of a constant temperature for the PCRV liner and concrete. This simplification is adequate only until failure of the PCRV insulation cover plates or failure of flow to the LCS.

In an extended UCHA, the insulation cover plates can begin failing about 10 h following a scram from full power with subsequent loss of all forced helium circulation. When the insulation cover plates fail, the insulation also falls away, exposing the 1.91-cm-thick PCRV liner to direct convective and radiative heat transfer. The PCRV concrete is in contact with the outer surface of the liner, so the cover plate failure would initiate a temperature transient in the concrete. The concrete temperature increase would be more severe if the normally running LCS were assumed to be inoperative.

To accurately characterize the temperature of an ∿3-m thickness of concrete, the temperature at different depths from the surface must be calculated by application of the heat conduction equation to subregions (nodes) within the concrete. The geometry of the PCRV concrete is approximated in slab geometry. The nodes would therefore be slabs of thickness small enough to ensure an accurate representation of the temperature profile. It is desirable to minimize the number of nodes to reduce the expense of the computation. Application of the analytical results of Ref. 2 resulted in the selection of a node thickness not exceeding about 3.8 cm. Uniform application of this requirement through the entire ∿3-m depth of the concrete would result in 79 nodes of equal thickness.

The transient calculation of 79 concrete temperatures would result in a significant increase in the overall computation cost for a long-term UCHA; therefore, a scheme using nodes of unequal thickness was investigated. For the innermost node, a thickness of 3.8 cm, as previously derived, was selected. Proceeding into the concrete away from the heated surface, the thickness of each succeeding node was increased (approximately doubled). Comparison of trial results revealed that a noding scheme using seven nodes of unequal thickness could adequately characterize the temperature transient in a UCHA. This noding structure works because the PCRV concrete is heated only at the inner surface. The small nodes at the inner surface are capable of responding rapidly to changes in the PCRV liner temperature; the larger interior nodes need not be capable of responding so rapidly because the rate of temperature increase is damped by the time it reaches them.

1.2 Development of the BLAST Steam Generator Code

J. C. Cleveland

A review was performed and comments were provided to Kernforschungsanlage (KFA) on the draft report "The Modified BLAST Code for Simulation of High-Temperature Reactor Steam Generator Dynamics." This report describes modifications to the ORNL BLAST code[3] made under KFA and Rheinisch Westfälischer Technischer Überwachungs Verein e.V. (RWTÜV) sponsorship.

Documentation was initiated to describe the current status of the BLAST steam generator code verification efforts. BLAST predictions are being compared by ORNL with steady state and dynamics data for the FSV reactor. BLAST results have also been compared by KFA and RWTÜV with data obtained from the Arbeitsgemeinschaft Versuchs Reaktor (AVR), a 15-MW(e) HTGR in Jülich, West Germany.

1.3 ORTURB Steam Turbine Code Development

J. C. Conklin

The ORTURB code[4] is a computer simulation to predict the dynamic response of the FSV steam turbines. Recent efforts were directed towards improving the physical modeling by comparing ORTURB predictions with actual plant data. Figure 1 presents a schematic drawing of the ORTURB computer modeling used for the FSV steam turbines.

On November 9, 1981, FSV was operating at 100% power [300 MW(e)] until 1 of 4 helium circulators tripped, causing 6 of 12 steam generators comprising 1 of 2 secondary coolant loops to be isolated with a corresponding generator load reduction to 50% power. The load was later reduced to 30%, and then the reactor was taken out of service for scheduled maintenance. The plant data logger recorded certain operating conditions of FSV during this transient, particularly parameters of interest for evaluating turbine and feedwater heater dynamic computer simulation performance.

The plant data for hot reheat steam temperature and pressure, feedwater flow to the steam generator, condensate feedwater pump discharge temperature, and condenser pressure were used as boundary conditions for the ORTURB simulation of the FSV plant transient of November 9, 1981. The ORTURB governing equation of turbine mass flow and pressure distribution determines the inlet flow for the intermediate- and low-pressure turbine (ILPT) from the hot reheat steam conditions and the pressure distribution in the turbine.

The plant data logger monitors the turbine extraction pressures and temperatures of the feedwater leaving each heater. Certain readings were obviously erroneous, such as a negative pressure for extraction points 6 and 7 (Fig. 1) or a constant pressure throughout the transient as recorded for all the extraction point temperatures and feedwater temperature leaving heater 5. Results were calculated for these parameters but are not presented.

Table 1 presents the ORTURB calculated pressures for the Fig. 1 extraction points 2–5 and the corresponding extraction pressures as recorded by the plant data logger. Table 2 presents the ORTURB results for the feedwater temperature leaving heaters 1–4 and 6 and the temperatures as recorded by the plant data logger. Figures 2 and 3 present the measured and computed extraction pressures and feedwater temperatures for heaters 6 and 3, respectively. The differences between the reported values at time zero are caused by differences between the heat balance data used to initialize ORTURB and those of the data logger, both for 100% power.

ORNL-DWG 80-5888 ETD

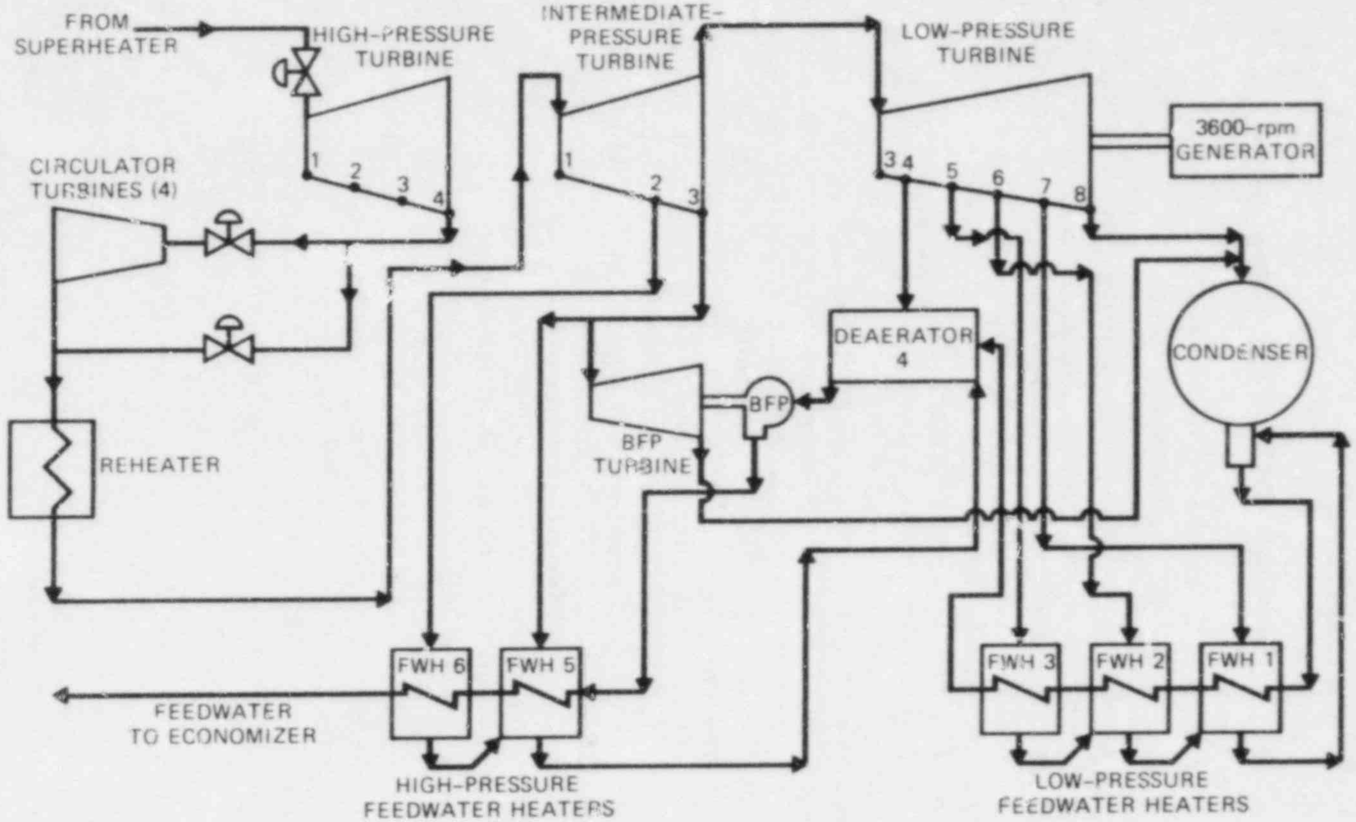

Fig. 1. FSV turbine generator plant diagram.

Table 1. Pressures for FSV turbine transient of November 9, 1981

Transient time (s)	Extraction point 5 Feedheater 3 [kPa (psia)]		Extraction point 4 Feedheater 4 [kPa (psia)]		Extraction point 3 Feedheater 5 [kPa (psia)]		Extraction point 2 Feedheater 6 [kPa (psia)]	
	Computed	Measured	Computed	Measured	Computed	Measured	Computed	Measured
0	182.0 (26.4)	169.6 (24.6)	555.7 (80.6)	601.2 (87.2)	1039.7 (150.8)	1107.3 (160.6)	1762.3 (255.6)	1758.2 (255.0)
30	140.0 (20.3)	128.9 (18.7)	430.2 (62.4)	485.4 (70.4)	749.5 (108.7)	779.1 (113.0)	1228.0 (178.1)	1225.5 (182.1)
60	120.0 (17.4)	104.1 (15.1)	366.1 (53.1)	423.3 (61.4)	637.8 (92.5)	661.9 (96.0)	1045.1 (151.7)	1071.4 (155.9)
90	115.8 (16.8)	98.6 (14.3)	351.6 (51.0)	415.1 (60.2)	612.9 (88.9)	645.3 (93.6)	1004.6 (145.7)	1051.5 (152.5)
120	113.1 (16.4)	95.1 (13.8)	342.7 (49.7)	408.9 (59.3)	597.8 (86.7)	635.0 (92.1)	981.8 (142.4)	1030.8 (149.5)
180	109.6 (15.9)	92.4 (13.4)	333.0 (48.3)	399.9 (58.0)	578.5 (83.9)	619.8 (89.9)	935.5 (138.3)	995.6 (144.4)
270	102.7 (14.9)	88.3 (12.8)	311.6 (45.2)	388.2 (56.3)	541.9 (78.6)	598.5 (86.8)	903.2 (131.0)	941.1 (136.5)
390	97.2 (14.1)	88.3 (12.8)	297.2 (43.1)	373.0 (54.1)	521.2 (75.6)	572.3 (83.0)	862.5 (125.1)	891.5 (129.3)
460	95.1 (13.8)	100.0 (14.5)	289.6 (42.0)	369.6 (53.6)	508.1 (73.7)	560.5 (81.3)	848.1 (123.0)	871.5 (126.4)

Table 2. Feedheater exit temperatures for FSV turbine transient of November 9, 1981

Transient time (s)	Feedheater 1 [°C (°F)]		Feedheater 2 [°C (°F)]		Feedheater 3 [°C (°F)]		Feedheater 4 [°C (°F)]		Feedheater 6 [°C (°F)]	
	Computed	Measured	Computed	Measured	Computed	Measured	Computed	Measured	Computed	Measured
0	71.9 (161.4)	66.7 (152.0)	93.4 (200.1)	90.0 (194.0)	112.6 (234.7)	107.7 (226.0)	153.3 (307.9)	153.9 (309.0)	204.1 (399.3)	203.9 (399.0)
30	69.6 (157.3)	67.8 (154.0)	91.5 (196.7)	88.9 (192.0)	108.6 (227.4)	107.2 (225.0)	152.1 (305.7)	153.9 (309.0)	190.5 (374.9)	203.9 (399.0)
60	65.4 (149.7)	63.3 (146.0)	86.0 (186.8)	83.9 (183.0)	102.9 (217.2)	101.1 (214.0)	150.7 (303.3)	152.8 (307.0)	183.2 (361.8)	197.8 (388.0)
90	64.0 (147.3)	57.8 (136.0)	83.8 (182.9)	77.8 (172.0)	101.7 (215.2)	95.0 (203.0)	149.2 (300.5)	148.3 (299.0)	181.2 (358.2)	189.4 (373.0)
120	63.0 (145.5)	54.4 (130.0)	82.8 (181.0)	74.4 (166.0)	100.6 (213.2)	90.6 (195.0)	147.6 (297.7)	145.6 (294.0)	180.2 (356.3)	186.7 (368.0)
180	62.2 (143.9)	52.2 (126.0)	81.9 (179.5)	71.7 (161.0)	99.6 (211.4)	87.8 (190.0)	144.7 (292.4)	138.9 (282.0)	178.7 (353.7)	185.0 (365.0)
270	60.9 (141.6)	51.7 (125.0)	80.2 (176.3)	70.0 (158.0)	97.7 (208.0)	85.6 (186.0)	140.5 (284.9)	130.6 (267.0)	176.6 (349.8)	183.3 (362.0)
390	59.9 (139.8)	49.4 (121.0)	78.8 (173.9)	68.9 (156.0)	96.3 (205.4)	85.6 (186.0)	135.8 (276.5)	125.6 (258.0)	174.4 (345.9)	181.1 (358.0)
460	59.5 (139.1)	50.0 (122.0)	78.3 (173.0)	77.8 (172.0)	95.8 (204.4)	93.3 (200.0)	133.1 (271.6)	128.9 (264.0)	173.7 (344.7)	180.0 (356.0)

ORNL-DWG 83-5494 ETD

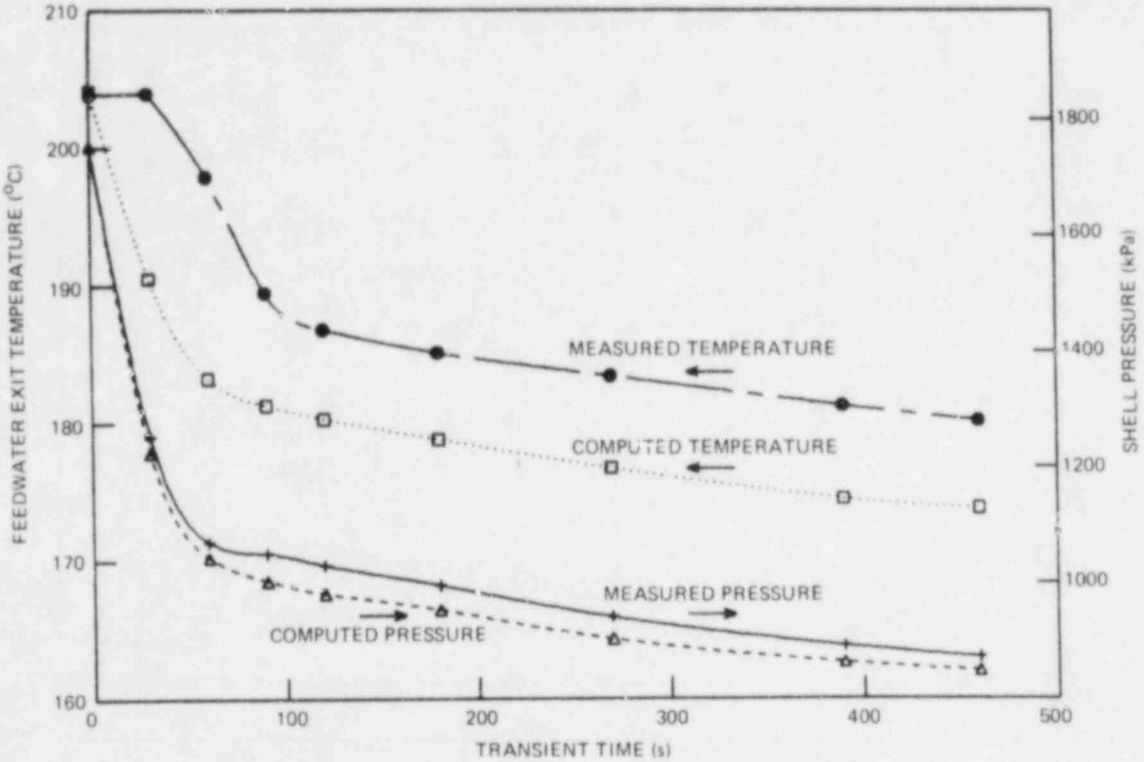

Fig. 2. Response of feedheater 6.

The error limits and response characteristics of these plant transducers for pressure and temperature would probably not be comparable with those of laboratory instruments. With this in mind, the agreement is reasonably good (∿10% difference for most values) over the first 460 s of the load reduction transient and particularly good (within 4%) for the extraction pressure of feedwater heater 6. Note, however, that the measured feedwater temperatures leaving heaters 1–3 and the measured pressure at extraction point 5 are significantly below those calculated by ORTURB for 90 to 390 s. This discrepancy is most likely caused by the uncertainty of the condensate feed pump mass flow rate. This important plant operating parameter is controlled at FSV to attempt to maintain a constant liquid level in the deaerator. However, the recorded value from the data logger could not be used in the simulation because it was obviously erroneous. The calculated values presented on Tables 1 and 2 and plotted on Figs. 2 and 3 resulted from a simulation where the deaerator liquid level was held constant throughout the computation, which would represent perfect controller response. In another computation, the condensate feedwater flow rate was arbitrarily increased over that needed to deliver a constant deaerator liquid level during the time period of interest, and results were more in agreement with those of the data logger.

An increase in deaerator liquid level was possible during this transient. The steam generator inlet feedwater flow rate was quickly

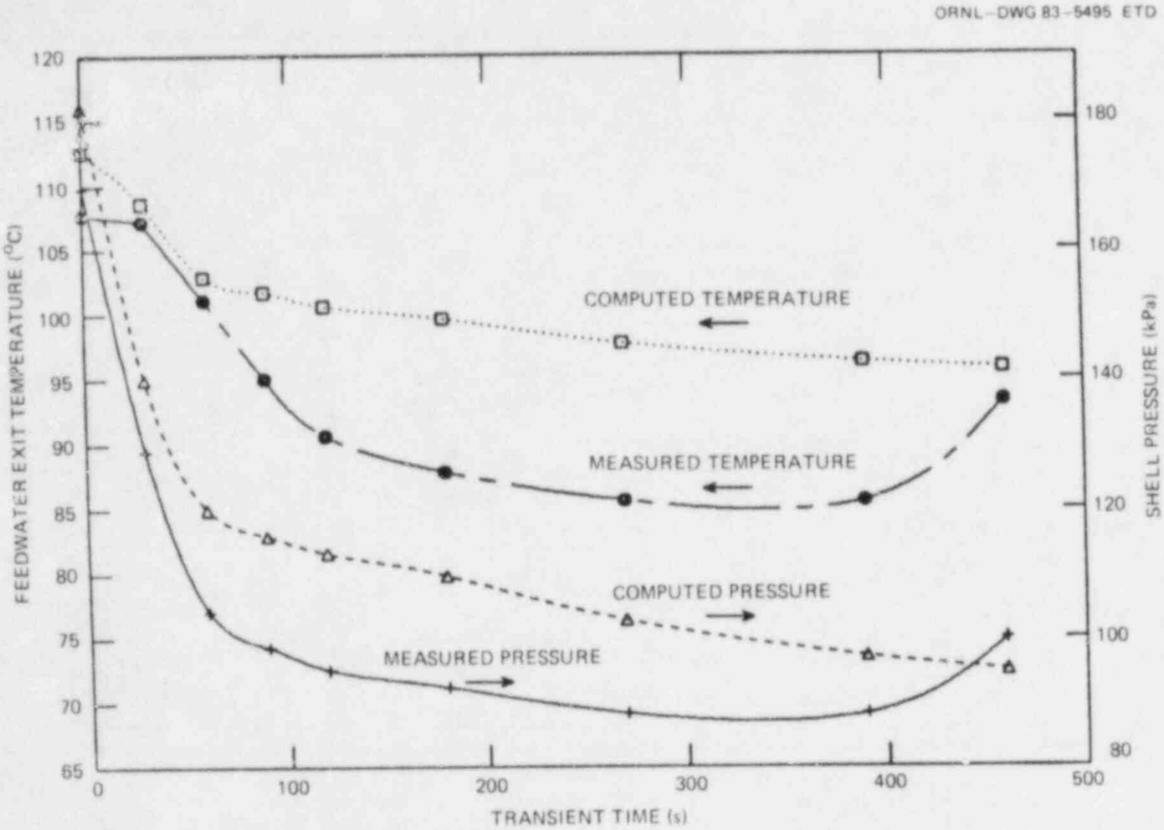

Fig. 3. Response of feedheater 3.

reduced to 50% of that required for full power, reflecting the isolation of one-half of the steam generators, while the condensate feedwater pumps were possibly still at the full-power operating point or coasting down from it. The tabulated results for the constant deaerator level case are still in reasonably good agreement with those of the data logger.

The calculated results for an actual plant transient at FSV agree reasonably well with those recorded by the plant data logger for the ILPT and feedwater heaters. These results justify the computational modeling and numerical solution used in the ORTURB code. Further information concerning the accuracy and response characteristics of the plant instrumentation transducers will be needed to account for the differences between calculated and measured values.

Further information concerning the accuracy and response characteristics of the transducers, and also any additional plant data logger information for other plant transients, has been requested from Public Service Company of Colorado.

These results shown on Figs. 2 and 3 as well as Tables 1 and 2, together with supporting details, were presented in a paper entitled "Dynamic Computer Simulation of the Fort St. Vrain Steam Turbines," which was published in the *Proceedings of the Fifth Power Plant Dynamics, Control and Testing Symposium*, Knoxville, Tenn., March 21–23, 1983.

1.4 Development of the ORECA Code for Simulating 2240-MW(t) SC/C HTGR Core Emergency-Cooling Transients

S. J. Ball

The ORECA code[1] three-dimensional core thermal-hydraulics dynamic simulation was adapted to the lower-power density (5.8-W/cm^3) version of the 2240-MW(t) Steam Cycle/Cogeneration (SC/C) Lead Plant design. This adaptation required only relatively minor changes in the higher-power density (7.2-W/cm^3) core model described previously.[5] The newer version corresponds to the General Atomic (GA) "Baseline Zero" design and is directly applicable to the Nuclear Regulatory Commission (NRC) siting study work involving ORNL, Brookhaven National Laboratory (BNL), Los Alamos National Laboratory (LANL), and Idaho National Engineering Laboratory (INEL).

In the newer version, there are 85 (vs 61) active core refueling regions in addition to the 24 side reflector regions. The top reflector-plenum element section, previously represented by a single axial node, was further subdivided into two nodes for the top reflector and a third for the plenum element. This gives a total of (85 + 24) x 14 = 1526 total nodes for the core. The plenum element model was adapted from the GA RECA-3 code,[6] which features a node point at the top surface to facilitate calculations of radiative heat transfer to the upper plenum. Improvements were also made in the core composite thermal conductivity algorithms to account for the decrease in effective radial conductivity that occurs at very high temperatures (2200°C).

A series of sensitivity studies were made in support of the siting study investigations. The first study addresses the question of when (or if) the PCRV will depressurize in a given UCHA scenario. A delayed depressurization would mean that the heat load on the upper-plenum cover plates and LCS would be much greater due to the high in-core convection flows carrying the heat upward, perhaps resulting in early failure of the cover plates and LCS. On the other hand, if the PCRV does not depressurize at all and LCS cooling is maintained (in spite of the loss of cover plates), the natural-convection leakage flow through the core auxiliary cooling system (CACS) and steam generators may cool the core enough to significantly reduce fuel damage. Two other related questions of interest are raised in this scenario. One concerns the probability that the system will remain pressurized. This probability will be much higher if the pressure relief valve successfully reseats when cycled about its 7.79-MPa (1130-psia) limit. This study assumes that the valve does not reseat and that once the 7.79-MPa limit is reached, the reactor depressurizes in 2 h. The other question is whether the hot bypass leakage flow through the CACS and steam generator loops might damage the loop components if sufficient cooling water were not available. This problem would have to be accounted for in the emergency operating procedures.

Sensitivity studies showed that combinations of relatively short (10 min) but non-zero main loop cooldown (MLCD) times, shutdown feed-water temperatures cooler than the reference value (204°C), and natural-circulation cooling from perhaps reasonable values of core bypass leakage path resistances may either delay depressurization or defer it indefinitely, at least for UCHAs in which the LCS is operational. Using a minimum-time MLCD, hot feedwater, and reference values of bypass leakage resistances, the primary system pressure reaches the 7.79-MPa relief valve limit in 1.5 h. If it is assumed that the MLCD is extended by about 10 min, the shutdown feedwater temperature is lowered from 204 to 149°C, and the three bypass loop resistances are arbitrarily set to be equivalent to single-region orifice openings of 25%, 40%, and 12%, respectively, then the system would not reach its relief valve pressure limit for 12.5 h. If it depressurized at this time, the calculations show that the assumed upper-plenum cover plate failure temperature of 816°C (1500°F) would be approached but not quite reached. With only one slight change in input assumptions (feedwater temperature = 121°C), however, upper-plenum cover plate failures begin at 14 h. With the additional heat rejection rate to the LCS due to removal of this liner insulation, the system does not depressurize at all, about 25% of the cover plates in the upper plenum eventually fail, and fuel damage is nil. Other reasonable combinations of assumed feedwater, MLCD, and leakage conditions yield estimates of depressurization times between 1.5 h and never. Note that plant operators would be working hard to restore cooling and that longer (or never) depressurization times would be much more likely than shorter ones. Thus, the possibility of cover plate failure cannot be neglected.

The rationale for assuming nonnegligible bypass flow is based on the fact that the gravity-operated butterfly isolation valves in the CACS and steam generator loops (1-m diam) will be subjected to extreme and torturous temperature conditions over several years and, during a postulated UCHA event, would not have any significant back pressure to seal them shut. Any significant warpage could result in leakage flows. While determining good values for these coefficients would be useful, one may also note that if means were provided to open the CACS or steam generator isolation valves somewhat during a UCHA, the benefits of this natural-circulation cooling could be realized. At the same time, however, some cooling water flow would have to be provided to prevent component damage.

Another uncertainty that affects the depressurization is the effectiveness of the LCS in providing primary system cooling during the periods of relatively stagnant primary flow (i.e., before depressurization). Based on the GA design, a considerable area subject to LCS cooling exists outside the core region. The reference case model assumes that these extended areas are very effective and, in the UCHA, are predicted to provide as much as 4 MW of cooling. In cases in which this assumed effectiveness was reduced, the time of depressurization was also decreased.

A second sensitivity study investigated the modeling and parameter assumptions for the radiant heat transfer from the core to the upper and lower plenums. In the previous model, ORECA represented the upper reflector and plenum elements with a single axial node (per region). This led to significantly higher estimates of heat loss by radiation to the upper-plenum cover plates and predicted earlier failure times for the cover plates. Data for emissivity e and absorptivity values for steel vary considerably, depending on conditions, from about 0.2 to 0.9 (Ref. 7). The reference value chosen was 0.8, which appeared to be typical of the nonshiny (oxidized) surfaces observed at FSV. However, because the surfaces are in a relatively oxygen-free atmosphere, a lower value of e may be possible. This case was tested in a run in which "thermal polishing" was assumed,[8] where the emissivities of the 61 inner refueling-region top surfaces and the upper-core sidewalls were assumed to fall from 0.8 to 0.2 when their temperatures reached ~816°C. The results indicated that, for the case of a UCHA in which the LCS was not operational, the thermal polishing effect delayed the time at which initial cover plate damage was predicted by about 10 h. Tests of the effects of including an algorithm for interreflected radiation within the upper and lower plenums showed that when the more detailed model was used (with e = 0.8), the heat load was distributed to the upper-plenum cover plates more evenly. Very little overall or long-range differences in core heatup rate or cover plate failure times were noted, however, so the simpler (and faster) model was used for the reference case runs.

The third study concerned the survivability of the core sidewall liner (and possibly the LCS) as a function of the effectiveness of the thermal shields and the emissivity. Because the four-layer shield members are spaced so close together, there was concern about how much attenuation would actually occur. If the shield were assumed to be a single-plane baffle, reducing the radiation to 0.5 of the no-shield value, the results indicated that cover plate failure would occur earlier in a UCHA that assumes LCS operation. The full value of shielding attenuation (0.2) is used as the reference value.

Another series of studies was done to determine the maximum time to restore cooling (MTRC). MTRC was originally defined by GA as the time in a UCHA at which the average fuel temperature reaches 1260°C (2300°F). The general idea was that if the core got any hotter, attempts to cool it with CACS forced circulation would result in damage by the hot coolant to downstream metal ducting, support structures, cooling tubes, and circulators. This damage would, in the long run, be more destructive than if the circulators were not used and if the core were cooled only by radiation heat transfer to the LCS. For the reference cases (with and without the LCS operational), the conventional MTRC was found to be typically 8.5 h.

More recently, GA introduced a second MTRC concept that is based on the idea that the MTRC can be determined from calculations of specific damage limits during the course of a postulated UCHA. The critical limits are (1) core auxiliary heat exchanger (CAHE) inlet helium temperature of 1093°C (2000°F) for 1 h or less and (2) an upper limit of 704°C (1300°F) on the CAHE tubing maximum temperature. The latter constraint was not a limiting factor in any of the simulations, because if it is assumed that CAHE coolant flow is maintained, the water-side heat transfer coefficient is much larger than that of the gas side. Thus, even with high inlet helium temperatures, the tube temperatures stay fairly close to the water temperatures and out of danger.

Several MTRC case variations were run; all assumed reactor scram and rapid cutoff of forced circulation at time zero and, for the reference case, assumed that the LCS continued operation. In all cases, the PCRV depressurized after about 1.5 h, so when forced circulation is resumed, low-pressure CACS operation is assumed. In the reference case with two CACSs available for restart, MTRC was limited to 12.5 h to prevent the CAHE inlet helium temperature from exceeding 1093°C for more than 1 h after CACS restart. In this case, as well as in all others involving variations in the number of CACS loops available, the results showed that if only one CACS were available, MTRC would be reduced by 1 h and if three CACS were available, MTRC could be extended by 1 h. Because the hot CAHE tube criterion was not critical, there was no advantage to reducing the CACS helium flow to cool down more gradually; in fact, such action was found to be counterproductive.

MTRC cases for temporary station blackouts (where the LCS also fails at time zero) were also run. The conventional MTRC limit (1260°C average fuel temperature) is again reached in 8.5 h. If it is assumed that two CACSs and the LCS are available for restart (with the PCRV depressurized), the MTRC is limited to 12 h to prevent the CAHE helium inlet temperature from exceeding 1093°C for more than 1 h. Here, as well as in the case where the LCS is operational, there is only negligible fuel damage (0.2%) due to the core heatup.

The feasibility of restarting only the LCS after longer outages was also investigated. In this case, the UCHA would result in considerable core damage, comparable to the long-term UCHA with an operational LCS, but would at least prevent ultimate containment failure. However, some concern remains about the feasibility of restarting the cooling water flow into the very hot liner because of the high thermal stresses that may be generated. Two variations of this case were run. In the first, it was determined that if the LCS were restarted within 40 h, it would be likely that the upper-plenum cover plates would survive and that the cooldown would proceed much the same as in the case where the LCS was available from the start. In the second case, the LCS was assumed to restart at a time just before the maximum liner temperature reached 816°C (time = 60 h). This limit was chosen because it is given as a limiting temperature for LCS restart in the FSV FSAR.[9] In this case, the upper-plenum cover plates fail shortly after LCS restart, but if it is assumed that the LCS does not fail in spite of the cover plate failures, ultimate containment failure would again be avoided.

A summary of some of the pertinent results from the MTRC studies is given in Table 3.

Another series of runs was made to consider variations of possible UCHA scenarios that include two LCS availability assumptions. The worst case, for permanent station blackout, assumes that the LCS and the CACS both fail at time zero and that cooling is never restored. PCRV depressurization occurs in about 1.5 h, and the LCS liners and concrete overheat rapidly. Water release from the PCRV concrete begins after about 4 h. The upper-core sidewall liner is predicted to fail after 48 h, and all of the top-head cover plates fail within the first 72 h. The time at which the PCRV liner ruptures and releases water and gas into the core region is not known. However, after 60 h some sidewall liner temperatures have reached 816°C with a considerable amount of water (steam) released behind the liner, so failure probably would have occurred at least by then. At that point, 31,750 kg of water (but no carbon dioxide) has

Table 3. Worst-case MTRC results

Time for 1260°C fuel average temperature, h	8
Time for CACS restart, h	
Limited by core outlet gas temperature >1093°C for <1 h	
With LCS	12.5
Without LCS	12
Time for LCS restart, h	
Limited to prevent upper-plenum cover plate failure	40
Limited by 816°C maximum liner temperature	60

been released; the rate of water release is 0.29 kg/s and the total fuel failure fraction determined from the GA (Goodin) time-at-temperature model[10] is 0.68. Within the next 8 h, carbon dioxide begins to be released, and the upper-plenum cover plates begin to fail. Shortly after these cover plates fail, the water release rate peaks at 0.35 kg/s. By the end of the 10-d (240-h) calculation, the water release rate has dropped to 0.24 kg/s. Conservative estimates of carbon dioxide release rates reach as high as 0.38 kg/s (for limestone concrete) during the transient.

At the end of the 10-d calculation station blackout period, a total of 200,000 kg of water and 118,000 kg of carbon dioxide has been released, the average fuel temperature has reached 3140°C and is still increasing, 100% of the fuel has failed, and most of the deterministic models used in ORECA have probably become invalid. The major results of the UCHA station blackout runs are summarized in Table 4.

The second UCHA transient assumes that there is no MLCD or CACS operation, but that the LCS continues to function in spite of boiling in the LCS cooling water system, relatively high liner temperatures, and significant water release from the PCRV concrete. PCRV depressurization occurs in about 1.5 h. The core continues to heat up, and after 44 h, the average fuel temperature reaches 2300°C and 50% of the fuel has failed.[10] The upper-core sidewall cover plate fails after 56 h, and shortly after that, the PCRV concrete water release rate peaks at 0.038 kg/s. After 144 h (6 d), the average fuel temperature reaches its maximum of 2820°C; just prior to that (128 h), the peak fuel temperature has reached its maximum of 3910°C. By the end of the 7-d calculated transient, the average fuel temperature was down to 2810°C, 88% of the fuel had failed, and the water release rate from the PCRV was 0.01 kg/s (total release = 7700 kg). No carbon dioxide release was predicted. Regarding the crucial question of whether the PCRV liner would have failed during this transient, the liner conditions are probably not

Table 4. UCHA results for station blackout (LCS not operational)

Depressurization time, h	1.5
Time for 50% fuel failure, h	42
Failure of most top-head cover plates, h	72
Failure of upper-core sidewall cover plates, h	48
At t = 240 h (10 d)	
Average fuel temperature, °C (°F)	3140 (5680)
Peak fuel temperature, °C (°F)	4010 (7250)
PCRV water release rate, kg/s (lb/h)	0.24 (1900)
Total PCRV water released, kg (lb)	197,000 (435,000)
PCRV CO_2 release rate, kg/s (lb/h)	0.066 (520)
Total CO_2 released, kg (lb)	120,000 (265,000)
Fuel failure, %	100

severe enough to cause failure. The peak temperature seen by the liners is only about 200°C.

A summary of the results of the UCHA with the LCS operation maintained is given in Table 5, and selected results for the two UCHA transients are shown in Figs. 4–6.

Table 5. UCHA results with LCS operational

Depressurization time, h	1.5
Time for 50% fuel failure, h	44
Failure of upper-core sidewall cover plates, h	56
Maximum average fuel temperature, °C (°F)	2820 (5110)
occurs at h	144
Maximum peak fuel temperature, °C (°F)	3910 (7075)
occurs at h	128
At t = 168 h (7 d)	
Average fuel temperature, °C (°F)	2810 (5090)
PCRV water release rate, kg/s (lb/h)	0.01 (80)
Total PCRV water released, kg (lb)	7,700 (17,000)
Total CO_2 released, kg (lb)	0 (0)
Fuel failure, %	88

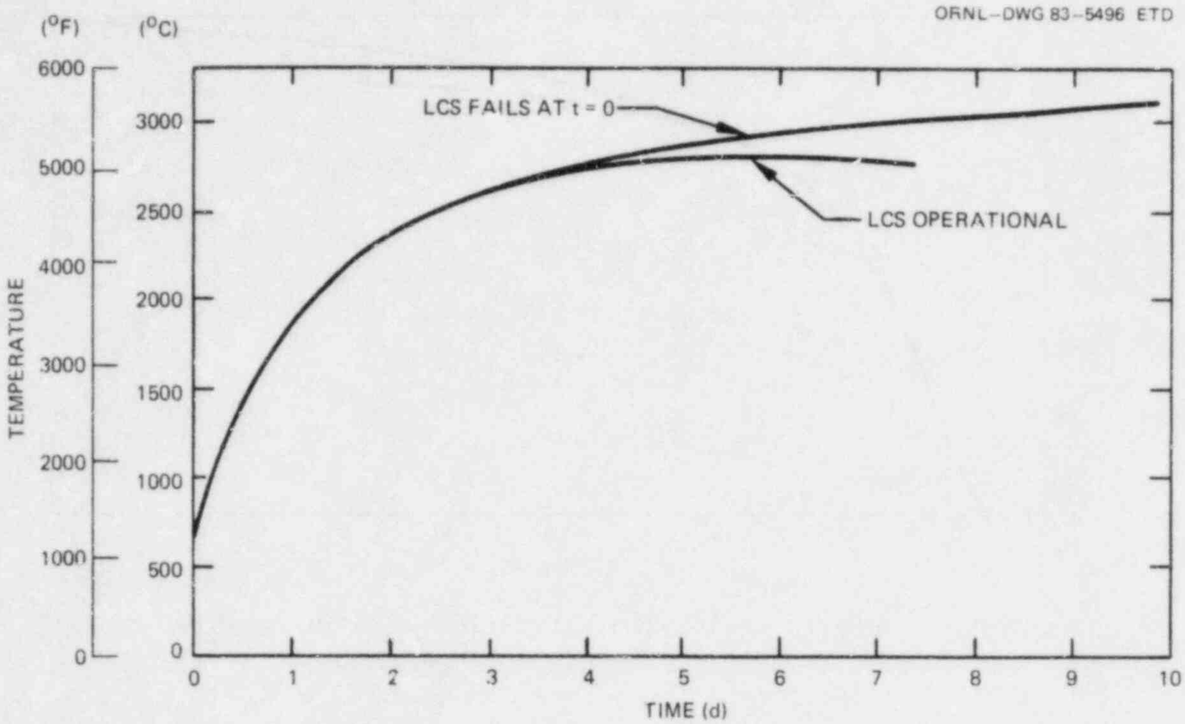

Fig. 4. UCHA-predicted fuel average temperature (5.8 W/cm^3 core).

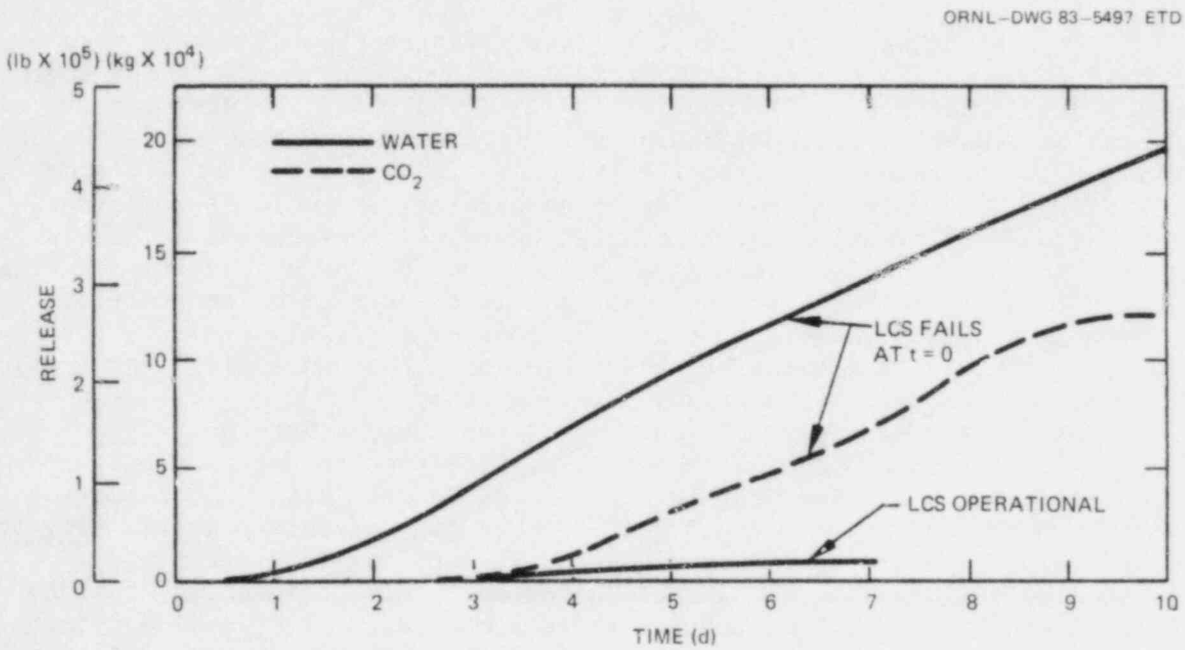

Fig. 5. UCHA-predicted water and CO_2 release from PCRV (5.8 W/cm^3 core).

ORNL-DWG 83-5493 ETD

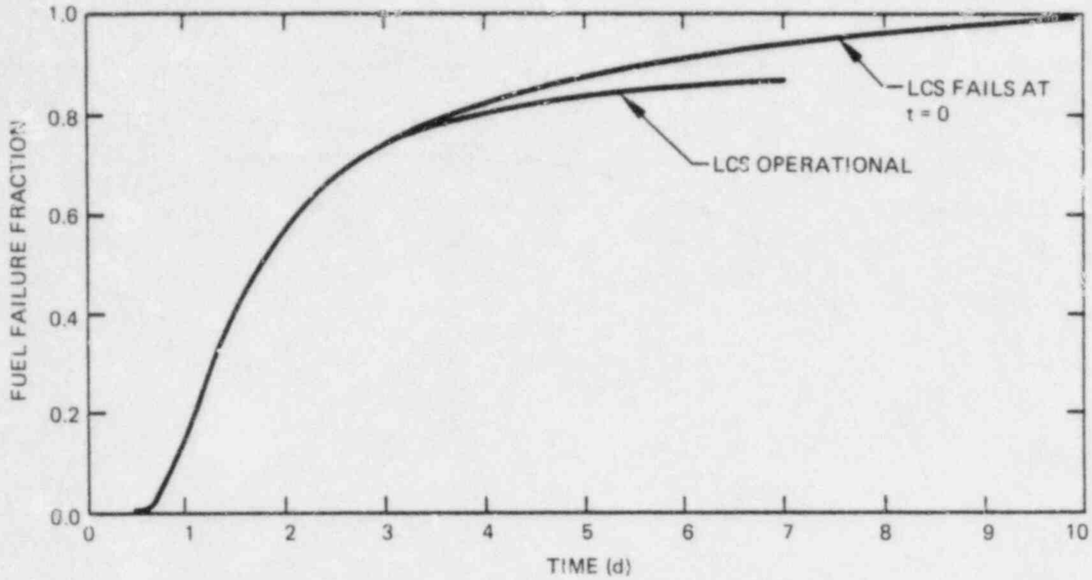

Fig. 6. UCHA-predicted fuel failure fraction (Goodin) (5.8 W/cm^3 core).

1.5 Fission Product Release from HTGRs

T. B. Lindemer

Equations were derived for the partial pressures of metal, metal oxide, and metal carbide gases at 2000 to 4000 K in the HTGR core under accident conditions. The species included those for the actinides, fission products, silicon, and boron. In the 2240-MW(t) core, there are about 3.4 moles of SiC (from the Triso coatings) per mole of actinide, and about 2.6 moles of boron (as boron carbide) per mole of actinide. Background information and a detailed description of the equation derivations and calculations are given in the following paragraphs. The results of these calculations were used in the design of the initial experimental apparatus for studies of loss of materials from the core during a UCHA. The equations and explanatory text were also sent to BNL in support of the 2240-MW(t) HTGR siting study.

In a 1974 GA report,[11] John Norman published equations for the partial pressures of metal and metal carbide species over actinide carbide fuel. However, the metal oxide gases must also be considered because of the presence of CO. The CO has two possible sources. One is the conversion of the ThO_2 and UO_2-UC_2 fuel to carbides after the coatings fail, giving 2 moles of CO for each mole of actinide dioxide. This generates enough CO to give a few atmospheres of CO in the primary circuit. The second CO source is the reaction of hot graphite with water (steam) introduced into the circuit if the LCS, and thus the liner, fails.

Several typical equilibria produce metal oxide gases in the uranium system,

$$UC_2\text{(solid, liquid)} + CO\text{(gas)} \rightleftarrows UO\text{(gas)} + 3C\text{(solid)},$$

$$UC_2\text{(solid, liquid)} + 2CO\text{(gas)} \rightleftarrows UO_2\text{(gas)} + 4C\text{(solid)}.$$

One could also write an equilibrium involving UO_3(gas), but it can be shown that the partial pressure is insignificant relative to either UO(gas) or UO_2(gas) under HTGR accident conditions.

The thermodynamic calculations were accomplished using standard procedures. The thermodynamic data needed for these calculations were generally obtained from standard data reference tables. Unknown data were estimated, again using techniques common to the field of chemical thermodynamics. For each equilibrium, the difference in the Gibbs free energy at temperature ΔG^o_T was calculated at 1500 and 3000 K from values of the standard enthalpy of formation of each species at 298.15 K, $\Delta H^o_{f,298}$, and the Gibbs free energy functions $(G^o_T - H^o_{298})/T$ at either 1500 or 3000 K. The ΔG^o_{1500} and ΔG^o_{3000} values were then fitted to an equation of the form $\Delta G^o_T = a + bT$. Again using the U-C-O system as an example, the metal oxide partial pressures can be calculated from the equations

$$P_{UO}(\text{atm}) = P_{CO}(\text{atm})\ e\left(\frac{a_1 + b_1\ T}{RT}\right),$$

and

$$P_{UO_2}(\text{atm}) = \left[P_{CO}\ (\text{atm})\right]^2\ e\left(\frac{a_2 + b_2\ T}{RT}\right).$$

in which R is 1.987 $\text{cal}\cdot\text{mol}^{-1}\cdot\text{K}^{-1}$. The coefficients a and b and the exponent on P_{CO} are given in Table 6. Also given are the partial pressures of each species at P_{CO} = 1 atm and at 2000, 2500, and 3000 K. The total pressure of all uranium-bearing gases is obtained by adding P_{UO} and P_{UO_2} to P_U and P_{UC_2} obtained from Norman's publication. To permit comparison of the partial pressures of the metal and metal carbide gases with the metal oxide gases, Norman's coefficients A_{VAP} and B_{VAP} were used to calculate the partial pressures shown in Table 6. His coefficients were also converted to the a and b values used here, where a = (-1000 R B_{VAP} ln 10) and b = (R A_{VAP} ln 10).

The coefficients in Table 6 should not be used to calculate partial pressures below 2000 K, because the T-P_{CO} conditions may be sufficient

Table 6. Coefficients for T > 2000 K and partial pressures[a,b]

Gaseous species[c]	Coefficients[c,d]			Partial pressures (atm) for P_{CO} = 1 atm at		
	m	a	b	2000 K	2500 K	3000 K
B	0	133753	-34.89	1.0E-7	8.6E-5	7.6E-3
B_2O	1	-50381	2.17	9.3E-6	1.2E-4	6.4E-4
BO	1	-27661	0.238	1.1E-3	4.3E-3	1.1E-2
B_2O_2	2	58835	-41.11	2.8E-3	1.5E-4	2.0E-5
B_2O_3	3	111184	-69.72	8.2E-4	3.0E-6	7.3E-8
Si	0	-122366	35.51	2.4E-6	1.2E-3	7.0E-2
SiO	1	-9312	-10.53	4.8E-4	7.7E-4	1.0E-3
Th	0	-164708	29.28	2.5E-12	1.0E-8	2.5E-6
ThC_2	0	-180264	35.96	1.4E-12	1.3E-8	5.3E-6
ThO	1	-47114	-5.74	4.0E-7	4.2E-6	2.1E-5
ThO_2	2	28152	-42.44	6.3E-7	1.5E-7	6.0E-8
U	0	-129479	20.59	2.0E-10	1.5E-7	1.2E-5
UC_2	0	-177062	36.10	3.5E-12	2.6E-8	9.8E-6
UO	1	-36793	-14.79	5.3E-8	3.4E-7	1.2E-6
UO_2	2	47692	-49.09	3.0E-6	2.8E-7	5.6E-8
Pu	0	-88302	15.78	6.3E-7	5.4E-5	1.0E-3
PuC_2	0	-137257	23.79	2.0E-10	1.6E-7	1.6E-5
PuO	1	-8414	-15.49	5.0E-5	7.6E-5	1.0E-4
Y	0	-118041	19.26	2.0E-9	7.8E-6	4.1E-5
YC_2	0	-179800	39.8	1.1E-11	9.6E-8	4.0E-5
YO	1	-34511	-7.57	3.8E-6	2.1E-5	6.8E-5
La	0	-119413	23.61	1.3E-8	5.2E-6	2.9E-4
LaC_2	0	-152355	35.73	1.4E-9	3.1E-6	5.1E-4
LaO	1	-9013	-9.18	1.0E-3	1.6E-3	2.2E-3
Ce	0	-134969	30.97	1.1E-8	9.3E-6	8.6E-4
CeC_2	0	-167911	44.97	3.0E-9	1.4E-5	4.0E-3
CeO	1	-1722	-12.00	1.5E-3	1.7E-3	1.8E-3
Eu	0	-53072	15.01	3.0E-3	4.4E-2	2.6E-1
EuC_2	0	-119871	30.47	3.6E-7	1.5E-4	8.4E-3
EuO	1	-19731	-13.82	6.7E-6	1.8E-5	3.5E-5
Nd	0	-89217	15.88	5.2E-7	4.7E-5	9.3E-4
NdC_2	0	-139087	32.03	6.3E-9	6.9E-6	7.4E-4
NdO	1	-2701	-13.59	5.4E-4	6.2E-4	6.8E-4
Pr	0	-100198	20.00	2.6E-7	4.1E-5	1.2E-3
PrC_2	0	-143204	34.68	8.5E-9	1.1E-5	1.4E-3
PrO	1	-1944	-13.10	8.4E-4	9.3E-4	9.9E-4
Sm	0	-63138	17.02	6.0E-4	1.6E-2	1.3E-1
SmO	1	-3138	-17.73	6.1E-5	7.1E-5	7.9E-5
Zr	0	-189872	35.00	7.9E-14	1.1E-9	6.6E-7
ZrC_2	0	-226016	43.01	5.0E-16	4.4E-11	8.6E-8
ZrO	1	-78171	-10.93	1.2E-11	6.0E-10	8.2E-9

[a]Also see Ref. 11 for the calculations for metal and metal carbide species.

[b]Not to be used as T < 2000 K.

[c]Coefficients for the metal and metal carbides were derived from Table I of Ref. 11, except for B and Si, which were derived in the present work.

[d]$P(atm) = [P_{CO}\ (atm)]^m\ e[(a+bT)/(1.987T)]$.

in some systems to result in the formation of stable condensed-phase oxides (ThO_2, B_2O_3, La_2O_3, SiO_2, UO_2, etc.) instead of the condensed-phase carbides. Partial pressures over the oxides would be calculated from a separate set of equations.

Species from the boron and silicon systems are also considered. Boron is present as B_4C in the neutron control material, while silicon originates from the SiC layer in the fuel particles. The molar ratio Si/(U+TH) in a reload HTGR core is $\sim$3.4:1, a significant amount of silicon.

Metal oxide and hydroxide species for the other FPs were also considered, but found to be unimportant under P_{CO} conditions likely to exist within the hot graphite core. Norman's data are thus complete for Cs, Rb, Ba, Sr, Mo, Tc, and Sb. The pressures of ruthenium and rhodium, already low, may be somewhat lower than Norman's values because of the formation of the very stable condensed-phase compounds URh_3 and URu_3. In the latter case, for example,

$$P_{Ru} = e\left(\frac{-165370 + 40.43T}{RT}\right) .$$

The maximum possible pressure of the FPs can be calculated via the equation $PV = nR_1T$. Clearly, if the total core inventory of a given FP has evaporated from the condensed phase, then it exists only in the gas phase, and the pressure can no longer follow the relationships given in Table 6. (The simplest case, of course, is for krypton and xenon.) The previous equation was evaluated for the maximum pressure in a reload fuel block (or, equivalently, in a reload fuel core), where the molar ratio C/Th $\gtrsim$ 600 and C/U $\gtrsim$ 850, which leads to (Th+U)/C = 0.00285. The term n for the FPs is equal to (fraction fima)(fraction yield) (0.00285). The term V is calculated from the volume of 1 mol of graphite and the void volume in the block. At theoretical density, the molar volume of carbon is $\gtrsim$5.3 cm^3/mol. The actual fuel block is comprised of coolant holes as well as graphite and fuel rods, both containing about 20% porosity, which leads to $\gtrsim$0.6 cm^3 void volume per 1 cm^3 theoretically dense graphite. The value of R_1 is 82.06 $cm^3 \cdot atm \cdot mol^{-1} \cdot K^{-1}$. Substitution leads to P(atm) = 0.073 (fraction fima)(fraction yield)(temperature in Kelvin). If the volume were considered to be the entire primary circuit, then the pressure would be about 0.1 of that calculated from the previous equation. Thus, for Kr + Xe at full burnup, the in-core P_{Kr+Xe} at 2500 K $\gtrsim$ 8.4 atm, whereas the P_{Kr+Xe} in the entire circuit at an average temperature of 1000 K would be $\gtrsim$0.34 atm. As far as the species in Table 6 are concerned, this equation limits the maximum in-core pressure of low-yield species such as europium.

The actual partial pressures may be lower than those calculated from the equations presented here and in Norman's report[11] because the thermodynamic chemical activity of the condensed phases may be less than the value of unity assumed here and by Norman. The chemical activity of each of the carbide-forming FPs would be lowered simply by assuming that each activity is that for the ideal solution of carbides formed by the actinide fuel (after it is converted to carbide) and the FPs. In the ideal case, the chemical activity is equal to the mole fraction and for a given FP is approximately (chemical activity) = (fraction yield) (fraction fima). This relation should be applicable to Ba, Sr, Nb, Zr, Mo, Y, and the lanthanides. The chemical activity would also be lowered in a generally unpredictable way by dissemination of the silicon, boron, actinides, and FPs in the core graphite. In the case of Cs, Rb, Sr, and Ba, the partial pressures are given in Norman's report[11] as a function of temperature and concentration in the graphite, although the data base is at $T < 2000$ K and is thus extrapolated to the accident temperatures.

1.6 Model and Code Development for Fission-Product Redistribution During Severe Accidents

I. Siman-Tov

The general mathematical methodology for modeling the FP redistribution in an HTGR core during a UCHA was established. Based on the assumptions outlined in the previous quarterly report,[5] which imply a one-dimensional (1-D) diffusion model in the fuel elements and a unidirectional steady axial gas flow model in the coolant channels with well-mixed conditions in the channels and plenums, the following set of equations was developed to represent the FP redistribution model.

The transient 1-D radial mass conservation equation in the fuel element regions is

$$\frac{\partial C}{\partial t} = \dot{Q} - \lambda C + \frac{1}{r}\frac{\partial}{\partial r}\left(r\ D\ \frac{\partial C}{\partial r}\right) , \tag{1}$$

where

- C = the concentration of FP for a particular group,
- $\dot{Q}$ = FP concentration produced through decay from parent FP,
- λ = decay constant of FP,
- D = mass diffusion coefficient for FP,
- r = represents an effective path from the fuel rod to the coolant channel in a plane perpendicular to the axial direction.

An initial condition for Eq. (1) is the FP inventory present in the fuel elements at the start of the accident. It is assumed that all structural components and coolant channels are free of FPs; that is, FPs present from failure and diffusion during normal operating conditions are considered negligible.

$$C_o = f\ (\tau,\lambda,\sigma) \quad \text{at } t = 0\ , \tag{2}$$

where

C_o = FP concentration at the onset of the accident,

t = time from onset of accident,

τ = time fuel has spent under normal operating conditions,
λ, σ= production and decay properties of the FP group.

The boundary condition at the solid-gas interface (r = R) is given by a mass-transfer correlation

$$\dot{M}_{sc} = hA\,(C_s - C_c) \quad \text{at } r = R\ , \tag{3}$$

where

$\dot{M}_{sc}$ = mass transfer rate from solid to coolant,
h = mass transfer coefficient,
A = cross-sectional area normal to mass transfer,
C_s = mass concentration on solid surface,
C_c = mass concentration in the gas free stream.

For symmetry reasons, the boundary condition at the center of the fuel element (r = 0) is $\frac{\partial C}{\partial r} = 0$.

Alternately, the boundary condition at r = R may also be expressed in terms of a correlation between the FP vapor pressures at the surface of the solid and in the bulk of the fluid. The vapor pressure differential will also determine the direction in which the FP moves (i.e., the FP may either be released from the surface or plated out on the surface).

The steady state continuity equation describes the axial steady fluid flow in the coolant channels. This choice is based on the assumption that the FPs are well mixed in the carrier gas and there is no appreciable holdup of the FPs in the channels. In terms of mass flow rates this becomes

$$\dot{M}_{in} + \dot{M}_{sc} = \dot{M}_{out}\ , \tag{4}$$

that is, FP inflow from upstream plus FP release from solid equals FP outflow to downstream.

For the cooling channels, the initial inventory of the FPs is zero. The boundary condition for the coolant channels at either end is a result of the instantaneously well-mixed assumption in both the top and lower plenums. The boundary conditions for channels with downflow from the upper plenum is based on the relation: the net total mass flow rate available for entering the downflow stream from the upper plenum equals the total mass flow rate coming from the upflow channels minus the total mass plateout rate on the structural materials in the plenum minus the total mass leakage rate out of the PCRV.

$$\dot{M}_{net} = \dot{M} - \dot{M}_p - \dot{M}_l\ , \tag{5}$$

and

$$\dot{M}_i = \dot{M}_{net}\, v_i / \Sigma v_i\ ,$$

where M_i is the mass flow rate entering the individual downflow channel i from the upper plenum, weighted by the velocity v_i of the carrier gas in that channel.

The boundary condition for channels with upflow starting at the bottom plenum is derived in the same manner.

A general mass balance of the FP is obtained by accounting for the total mass generated, the total mass decayed, and the total mass that left the PCRV up to time t.

$$M = M_q - M_d - M_l \quad , \tag{6}$$

where

M = the total mass of a FP in the model present at time t,
M_q = the total mass generated by birth from parents up to time t,
M_d = the total mass decayed up to time t,
M_l = the total mass leakage out of the PCRV up to time t.

M also must be equal to the sum of the masses of the FP present at time t in the individual volumes considered in the numerical model:

$$M = \sum_{\text{all } j} m_j \quad , \tag{7}$$

where m_j is the mass of FP present in an individual volume element j at time t.

These last two conditions provide a basis for testing the procedure, because in both cases the total mass of a given FP in the model has to be the same irrespective of the method of calculation.

Note that the equations presented here solve the FP redistribution problem independently for each FP group. This assumes no chemical or thermodynamic interactions between members of different groups. This has to be a basic consideration in the construction of FP groups.

The development of the given general formulation into a specific working model, which has to be compatible with the geometry and node structure of the ORECA code, has been divided into several tasks: (1) surveying and compiling information on the initial inventory of FPs at the onset of a UCHA; (2) sorting the FPs into different groups based on their transport behavior in the fuel elements; (3) compiling thermal, mass transport, and nuclear properties for all members of the different groups, and then developing effective properties for each of the FP groups; (4) developing a volumetric heat generation equivalent to FP concentration (besides keeping track of FPs that have significance other than as a heat source); and (5) integrating this information into the solution of the mass transport of the FPs in the fuel elements considering the three principal modes of FP behavior: volatiles where the diffusion is assumed instantaneous; stationaries ($D = 0$), where the FPs stay in the fuel elements; and mobiles, where both the diffusion coefficients D and the vapor pressures need to be known. Additional tasks may evolve in the process of handling the specifics of the model and code development.

2. MEETINGS AND TRIPS UNDER PROGRAM SPONSORSHIP

2.1 HTGR Siting Study Meeting at ORNL, January 26–28, 1983

S. J. Ball J. C. Conklin
R. M. Harrington T. B. Lindemer
I. Siman-Tov

Discussions were held with siting study group participants from NRC, BNL, and INEL on problems with completing the report on the 2240-MW(t) lead plant source term.

2.2 Visit to GA Technologies, San Diego, Calif., February 16–17, 1983

T. B. Lindemer

Discussions were held with NRC, BNL, GA Technologies, and INEL personnel on the models and assumptions used in the FP release and transport calculations for postulated severe accidents.

2.3 Fifth Power Plant Dynamics, Control, and Testing Symposium, Knoxville, Tenn., March 21–23, 1983

S. J. Ball J. C. Conklin
R. M. Harrington

The meeting topics covered the latest modeling and verification techniques used in reactor and other power plant dynamics. J. C. Conklin presented a paper entitled "Dynamic Computer Simulation of the Fort St. Vrain Steam Turbines."

REFERENCES

1. S. J. Ball, *ORECA-I: A Digital Computer Code for Simulating the Dynamics of HTGR Cores for Emergency Cooling Analysis*, ORNL/TM-5159, Union Carbide Corp. Nuclear Div., Oak Ridge Natl. Lab., April 1976.

2. S. J. Ball, *Approximate Models for Distributed-Parameter Heat Transfer Systems, ISA Trans* 3(1), 38-47, January 1964.

3. R. A. Hedrick and J. C. Cleveland, *BLAST: A Digital Computer Program for the Dynamic Simulation of the High-Temperature Gas-Cooled Reactor Reheater Steam Generator Module*, ORNL/NUREG/TM-38, Union Carbide Corp. Nuclear Div., Oak Ridge Natl. Lab., August 1976.

4. J. C. Conklin, *ORTURB: A Digital Computer Code to Determine the Dynamic Response of the Fort St. Vrain Reactor Steam Turbines*, ORNL/NUREG/TM-399, Union Carbide Corp. Nuclear Div., Oak Ridge Natl. Lab., March 1981.

5. S. J. Ball et al., *HTGR Safety Studies for the Division of Accident Evaluation Quart. Prog. Rep., October 1–December 31, 1982*, ORNL/NUREG/TM-8443/V4.

6. J. F. Petersen, *RECA3: A Computer Code for Thermal Analysis of HTGR Emergency Cooling Transients*, GA-A14520, General Atomic Technologies, August 1977.

7. R. E. Rolling and A. I. Funai, *Investigation of the Effects of Surface Conditions on the Radiant Properties of Metals*, AFML-TR-64-363, part II, Lockheed Missiles and Space Company, April 1967.

8. Oak Ridge National Laboratory, *GCFR Annual Report for 1977*, ORNL-5246, Union Carbide Corp. Nuclear Div., Oak Ridge Natl. Lab., pp. 11-15, August 1978.

9. *Fort St. Vrain Nuclear Generating Station Final Safety Analysis Report*, Public Service Company of Colorado.

10. D. T Goodin, "Accident Condition Performance of HTGR Fuels," Document No. 906611 (Issue A), General Atomic Technologies, Inc., December 1982.

11. J. H. Norman, *Review of Vapor Pressures and Diffusion Coefficients of Certain HTGR Core Materials and Fission Products for Use in Reactor Accident Calculations*, GA-A12634, General Atomic Technologies, Inc., May 1974.

NUREG/CR-3492
Volume 1
ORNL/TM-8921/V1
Dist. Category R8

Internal Distribution

1-5. S. J. Ball
6. N. E. Clapp
7-11. J. C. Cleveland
12-16. J. C. Conklin
17-18 D. S. Griffith
19-23. R. M. Harrington
24. P. R. Kasten
25. A. D. Kelmers
26. T. S. Kress
27. T. B. Lindemer
28. A. P. Malinauskas
29. D. L. Moses
30. J. P. Sanders
31. I. Siman-Tov
32. R. S. Stone
33. H. E. Trammell
34. R. P. Wichner
35. ORNL Patent Office
36. Central Research Library
37. Document Reference Section
38-39. Laboratory Records Department
40. Laboratory Records, RC

External Distribution

41-44. Director, Office of Nuclear Regulatory Research, Nuclear Regulatory Commission, Washington, DC 20555
45. Chief, Advanced Safety Technology Branch, Division of Accident Evaluation, Office of Nuclear Regulatory Research, Nuclear Regulatory Commission, Washington, DC 20555
46. Office of Assistant Manager for Energy Research and Development, DOE, ORO, Oak Ridge, TN 37831
47-48. Technical Information Center, DOE, Oak Ridge, TN 37831
49-248. Given distribution as shown in category R8 (10-NTIS)

NRC FORM 335 (11-81)

U.S. NUCLEAR REGULATORY COMMISSION

BIBLIOGRAPHIC DATA SHEET

1. REPORT NUMBER (Assigned by DDC)
NUREG/CR-3492, Volume 1
ORNL/TM-8921/V1

2. (Leave blank)

3. RECIPIENT'S ACCESSION NO.

4. TITLE AND SUBTITLE (Add Volume No., if appropriate)
High-Temperature Gas-Cooled Reactor Safety Studies for the Division of Accident Evaluation Quarterly Progress Report, January 1 - March 31, 1983

5. DATE REPORT COMPLETED

MONTH	YEAR
October	1983

DATE REPORT ISSUED

MONTH	YEAR

6. (Leave blank)

7. AUTHOR(S)
S. J. Ball, J. C. Cleveland, J. C. Conklin,
R. M. Harrington, T. B. Lindemer, I. Siman-Tov

8. (Leave blank)

9. PERFORMING ORGANIZATION NAME AND MAILING ADDRESS (Include Zip Code)
Oak Ridge National Laboratory
P. O. Box X
Oak Ridge, Tennessee 37831

10. PROJECT/TASK/WORK UNIT NO.

11. FIN NO.
B0122

12. SPONSORING ORGANIZATION NAME AND MAILING ADDRESS (Include Zip Code)
Division of Accident Evaluation
Office of Nuclear Regulatory Research
U. S. Nuclear Regulatory Commission
Washington, D.C. 20555

13. TYPE OF REPORT
Quarterly

PERIOD COVERED (Inclusive dates)
January 1 - March 31, 1983

14. (Leave blank)

15. SUPPLEMENTARY NOTES

16. ABSTRACT (200 words or less)

Work continued on high-temperature gas-cooled reactor safety research directed towards both the Fort St. Vrain and 2240-MW(t) lead plant reactors. Code development and verification activities addressed simulations of unrestricted core heatup accidents, steam generator and turbine-plant perturbations, and fission-product redistribution during severe accidents. Analyses and sensitivity studies of the lead plant thermal response were made for postulated severe accidents, and partial pressures of pertinent reactor materials were calculated for the resulting severe accident environment.

17. KEY WORDS AND DOCUMENT ANALYSIS

17a. DESCRIPTORS

17b. IDENTIFIERS/OPEN-ENDED TERMS

18. AVAILABILITY STATEMENT
Unlimited

19. SECURITY CLASS (This report)
Unclassified

20. SECURITY CLASS (This page)
Unclassified

21. NO. OF PAGES

22. PRICE
$

NRC FORM 335 (11-81)

120555078877 1 1AN1R6
US NRC
ADM-DIV OF TIDC
POLICY & PUB MGT BR-PDR NUREG
W-501
WASHINGTON DC 20555